Model reduction of conservation laws: nonlinear approximations and optimal projection

Tommaso Taddei, Inria Team MEMPHIS

Workshop on Uncertainty Quantification for High-Dimensional Problems
Amsterdam, November, 2024

Collaborators: N Barral, A Del Grosso, A Iollo, I Tifouti (Inria).
Sponsors: AEx Inria, EDF, Onera (Chaire PROVE).

Model reduction of parametric conservation laws

- Least-square Petrov-Galerkin projection
- Lagrangian approximations

Model reduction of parametric PDEs (I)

Motivation: develop effective simulation tools for *many-query* and *real-time* problems that involve solutions to parameterized PDEs:

- parameter sweeps;
- design and optimization;
- uncertainty quantification.

Model order reduction (MOR) aims to reduce the *marginal cost* to solve parametric PDEs, for real-time and many-query problems.

Model reduction of parametric PDEs (I)

Motivation: develop effective simulation tools for *many-query* and *real-time* problems that involve solutions to parameterized PDEs:

- parameter sweeps;
- design and optimization;
- uncertainty quantification.

Model order reduction (MOR) aims to reduce the *marginal cost* to solve parametric PDEs, for real-time and many-query problems.

Aim of the talk: review main features and recent advances of projection-based MOR methods for conservation laws.

Model reduction of parametric PDEs (II): offline/online decomposition

Consider the problem: find $u_\mu \in \mathcal{X} \ : \ R_\mu(u_\mu, v) = 0, \forall\, v \in \mathcal{Y}, \qquad \mu \in \mathcal{P}.$

We seek approximations of the form $\widehat{u}_\mu = Z(\widehat{\alpha}_\mu)$, with reduced order basis (ROB) $Z : \mathbb{R}^n \to \mathcal{X}$ and *generalized coordinates* $\widehat{\alpha} : \mathcal{P} \to \mathbb{R}^n$.

Model reduction of parametric PDEs (II): offline/online decomposition

Consider the problem: find $u_\mu \in \mathcal{X} \ : \ R_\mu(u_\mu, v) = 0, \forall\, v \in \mathcal{Y}, \qquad \mu \in \mathcal{P}.$

We seek approximations of the form $\widehat{u}_\mu = Z(\widehat{\alpha}_\mu)$, with reduced order basis (ROB) $Z : \mathbb{R}^n \to \mathcal{X}$ and *generalized coordinates* $\widehat{\alpha} : \mathcal{P} \to \mathbb{R}^n$.

Offline/training stage: (performed once)

1. estimate $u_{\mu^1}, \ldots, u_{\mu^{n_{\text{train}}}}$ using a FE (or FV...) solver;
2. construct the ROB $Z : \mathbb{R}^n \to \mathcal{X}$;
3. construct a parametric reduced-order model (ROM) for $\widehat{\alpha}$.

Online/prediction stage: (performed for any new $\mu \in \mathcal{P}$)

1. compute $\widehat{\alpha}_\mu$ using the ROM;
2. return the state estimate $\widehat{u}_\mu = Z(\widehat{\alpha}_\mu)$.

A concrete example: POD-Galerkin method of nonlinear elasticity problems (I)

Consider the problem $-\nabla \cdot P_p(\nabla u_\mu) = 0$ with suitable BCs.

$P_p(\nabla u_\mu)$ Piola-Kirchhoff tensor;

$\mu = [p, \bar{\sigma}]$ vector of parameters;

$\bar{\sigma}$= traction, p material properties.

Goal: speed up evaluation of $\mu \mapsto u_\mu$

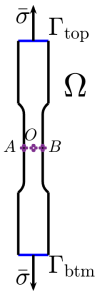

A concrete example: POD-Galerkin method of nonlinear elasticity problems (I)

Consider the problem $-\nabla \cdot P_p(\nabla u_\mu) = 0$ with suitable BCs.

$P_p(\nabla u_\mu)$ Piola-Kirchhoff tensor;

$\mu = [p, \bar{\sigma}]$ vector of parameters;
$\bar{\sigma}$= traction, p material properties.

Goal: speed up evaluation of $\mu \mapsto u_\mu$

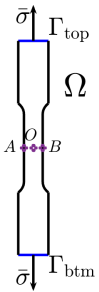

Step 0: introduce the FE discretization: find $u_\mu^{\text{hf}} \in \mathcal{X}_{\text{hf}} \; : \; R_\mu(u_\mu^{\text{hf}}, v) = 0, \quad \forall\, v \in \mathcal{X}_{\text{hf}}$

Step 1: generate snapshots using the FE model: $\mathcal{S} := \{u_\mu^{\text{hf}} : \mu \in \mathcal{P}_{\text{train}}\}$;

Step 2: generate the linear ROB $Z = [\zeta_1, \ldots, \zeta_n]$ using POD (=weighted SVD).

Step 3: generate the Galerkin ROM $R_\mu(Z(\widehat{\alpha}_\mu), \zeta_i) = 0$ for $i = 1, \ldots, n$.

A concrete example: POD-Galerkin method of nonlinear elasticity problems (II)

Representative performance: FEM with $N = 22369$ dofs, ROM with $n = 10$ dofs, $\#\mathcal{P}_{\text{train}} = 20$.

Relative H^1 error (over test set): $\approx 6 \cdot 10^{-4}$, speed up (avg): ≈ 1300.

Non-intrusive (POD+RBF): error: ≈ 0.13, speed up (avg): ≈ 1500.

A concrete example: POD-Galerkin method of nonlinear elasticity problems (II)

Representative performance: FEM with $N = 22369$ dofs, ROM with $n = 10$ dofs, $\#\mathcal{P}_{\text{train}} = 20$.

Relative H^1 error (over test set): $\approx 6 \cdot 10^{-4}$, speed up (avg): ≈ 1300.

Non-intrusive (POD+RBF): error: ≈ 0.13, speed up (avg): ≈ 1500.

The ROM is effective because

- the solution set is well-approximated by a low-dimensional linear space;
- Galerkin projection achieves near-optimal performance.

Speed up is achieved by

- reducing the dimensionality of the problem, $n \ll N$;
- improving the initialization of the nonlinear solver;
- resorting to a specialized sparse quadrature rule.

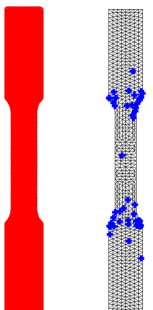

Extension to conservation laws: challenges and proposed solution

The extension of model reduction techniques to steady conservation laws is challenging.

- Galerkin projection typically leads to unstable ROMs.
- Linear ROBs and static meshes are ill-suited for transport phenomena.
- Presence of nonlinearities hinders benefits of dimensionality reduction.

Extension to conservation laws: challenges and proposed solution

The extension of model reduction techniques to steady conservation laws is challenging.

- Galerkin projection typically leads to unstable ROMs.
- Linear ROBs and static meshes are ill-suited for transport phenomena.
- Presence of nonlinearities hinders benefits of dimensionality reduction.

The past decade has witnessed major advances on the treatment of advection-dominated problems.

- (Least-square) Petrov-Galerkin projection.
- Nonlinear approximation methods.
- Effective hyper-reduction schemes for the treatment of nonlinearities.

Extension to conservation laws: challenges and proposed solution

The extension of model reduction techniques to steady conservation laws is challenging.

- Galerkin projection typically leads to unstable ROMs.
- Linear ROBs and static meshes are ill-suited for transport phenomena.
- Presence of nonlinearities hinders benefits of dimensionality reduction.

The past decade has witnessed major advances on the treatment of advection-dominated problems.

- **(Least-square) Petrov-Galerkin projection.**
- **Nonlinear approximation methods.**
- Effective hyper-reduction schemes for the treatment of nonlinearities.

Farhat et al, 2015; Yano, Patera, 2018,...

Model reduction of parametric conservation laws

- Least-square Petrov-Galerkin projection
- Lagrangian approximations

Definitions and notation

We introduce the bases $\{\xi_i\}_{i=1}^N$ and $\{\nu_i\}_{i=1}^N$ of $\mathcal{X}$ and $\mathcal{Y}$.

Definitions and notation

We introduce the bases $\{\xi_i\}_{i=1}^N$ and $\{\nu_i\}_{i=1}^N$ of $\mathcal{X}$ and $\mathcal{Y}$.

- $u \in \mathcal{X}, v \in \mathcal{Y} \leftrightarrow \boldsymbol{u}, \boldsymbol{v} \in \mathbb{R}^N$, $u = \sum_{i=1}^N (\boldsymbol{u})_i \xi_i, v = \sum_{i=1}^N (\boldsymbol{v})_i \nu_i$;
- $F \in \mathcal{Y}' \leftrightarrow \boldsymbol{F} \in \mathbb{R}^N$, $F(v) = \boldsymbol{F}^\top \boldsymbol{v} \quad \forall\, \boldsymbol{v} \in \mathbb{R}^N$;

Definitions and notation

We introduce the bases $\{\xi_i\}_{i=1}^N$ and $\{\nu_i\}_{i=1}^N$ of $\mathcal{X}$ and $\mathcal{Y}$.

- $u \in \mathcal{X}, v \in \mathcal{Y} \leftrightarrow \boldsymbol{u}, \boldsymbol{v} \in \mathbb{R}^N$, $u = \sum_{i=1}^N (\boldsymbol{u})_i \xi_i, v = \sum_{i=1}^N (\boldsymbol{v})_i \nu_i$;
- $F \in \mathcal{Y}' \leftrightarrow \boldsymbol{F} \in \mathbb{R}^N$, $F(v) = \boldsymbol{F}^\top \boldsymbol{v} \quad \forall\, \boldsymbol{v} \in \mathbb{R}^N$;
- $(\cdot,\cdot)_{\mathcal{X}}, (\cdot,\cdot)_{\mathcal{Y}} \leftrightarrow \boldsymbol{X}, \boldsymbol{Y} \in \mathbb{R}^{N\times N}$,
$$(u,v)_{\mathcal{X}} = \boldsymbol{v}^\top \boldsymbol{X} \boldsymbol{u}, \quad (w,z)_{\mathcal{Y}} = \boldsymbol{z}^\top \boldsymbol{Y} \boldsymbol{w};$$
- $R_\mu(u_\mu, v) = 0 \;\; \forall\, v \in \mathcal{Y} \leftrightarrow \boldsymbol{R}_\mu(\boldsymbol{u}_\mu) = 0$;
- $DR_\mu[u_\mu] : \mathcal{X} \times \mathcal{Y} \to \mathbb{R} \leftrightarrow \boldsymbol{J}_\mu[\boldsymbol{u}_\mu] \in \mathbb{R}^{N\times N}$.

Definitions and notation

We introduce the bases $\{\xi_i\}_{i=1}^N$ and $\{\nu_i\}_{i=1}^N$ of $\mathcal{X}$ and $\mathcal{Y}$.

- $u \in \mathcal{X}, v \in \mathcal{Y} \leftrightarrow \boldsymbol{u}, \boldsymbol{v} \in \mathbb{R}^N$, $u = \sum_{i=1}^N (\boldsymbol{u})_i \xi_i, v = \sum_{i=1}^N (\boldsymbol{v})_i \nu_i$;
- $F \in \mathcal{Y}' \leftrightarrow \boldsymbol{F} \in \mathbb{R}^N$, $F(v) = \boldsymbol{F}^\top \boldsymbol{v} \quad \forall\, \boldsymbol{v} \in \mathbb{R}^N$;
- $(\cdot,\cdot)_{\mathcal{X}}, (\cdot,\cdot)_{\mathcal{Y}} \leftrightarrow \boldsymbol{X}, \boldsymbol{Y} \in \mathbb{R}^{N\times N}$,
$$(u,v)_{\mathcal{X}} = \boldsymbol{v}^\top \boldsymbol{X} \boldsymbol{u}, \quad (w,z)_{\mathcal{Y}} = \boldsymbol{z}^\top \boldsymbol{Y} \boldsymbol{w};$$
- $R_\mu(u_\mu, v) = 0 \ \ \forall\, v \in \mathcal{Y} \leftrightarrow \boldsymbol{R}_\mu(\boldsymbol{u}_\mu) = 0$;
- $DR_\mu[u_\mu] : \mathcal{X} \times \mathcal{Y} \to \mathbb{R} \leftrightarrow \boldsymbol{J}_\mu[\boldsymbol{u}_\mu] \in \mathbb{R}^{N\times N}$.

- The choice of $\boldsymbol{X}$ reflects the target norm of interest (L^2, H^1,...).
- The choice of $\boldsymbol{Y}$ should be designed to maximize stability.

Minimum residual formulation

We introduce the low-rank approximation: $\widehat{u}_\mu = Z\widehat{\alpha}_\mu$. where $Z = [\zeta_1, \ldots, \zeta_n] : \mathbb{R}^n \to \mathcal{X}$ is a linear operator.

The extension to affine approximations $\widehat{u}_\mu = \bar{u}_\mu + Z\widehat{\alpha}_\mu$ is trivial.

Our point of departure is the minimum residual formulation:

$$\min_{\alpha \in \mathbb{R}^n} \left(\sup_{v \in \mathcal{Y}} \frac{R_\mu(Z\alpha\,,\, v)}{\|v\|_{\mathcal{Y}}} \right) = \min_{\alpha \in \mathbb{R}^n} \| \boldsymbol{Y}^{-1/2} \boldsymbol{R}_\mu \left(\boldsymbol{Z} \alpha \right) \|_2.$$

Refs: Maday et al., 2003; Yano, 2014 (*minimum residual MOR*); Grimberg et al., 2021 (*reduced quadrature rules*).

Minimum residual formulation

We introduce the low-rank approximation: $\widehat{u}_\mu = Z\widehat{\alpha}_\mu$. where $Z = [\zeta_1, \ldots, \zeta_n] : \mathbb{R}^n \to \mathcal{X}$ is a linear operator.

The extension to affine approximations $\widehat{u}_\mu = \bar{u}_\mu + Z\widehat{\alpha}_\mu$ is trivial.

Our point of departure is the minimum residual formulation:

$$\min_{\alpha \in \mathbb{R}^n} \left(\sup_{v \in \mathcal{Y}} \frac{R_\mu(Z\alpha\,,\, v)}{\|v\|_{\mathcal{Y}}} \right) = \min_{\alpha \in \mathbb{R}^n} \| \boldsymbol{Y}^{-1/2} \boldsymbol{R}_\mu\,(\boldsymbol{Z}\alpha) \|_2.$$

- The ROM is online-efficient only for parametrically-affine problems.
- Application of reduced quadrature rules is possible if $\boldsymbol{Y}$ is diagonal.

Refs: Maday et al., 2003; Yano, 2014 (*minimum residual MOR*); Grimberg et al., 2021 (*reduced quadrature rules*).

Approximate minimum residual formulation ([TT, Zhang, 2021])

We introduce two successive approximations:

1. we replace $\sup_{v \in \mathcal{Y}}(\cdot)$ with $\sup_{v \in \mathcal{W}}(\cdot)$ where $\mathcal{W} = \operatorname{span}\{\psi_i\}_{i=1}^m$.

$$\min_{\alpha \in \mathbb{R}^n} \left(\sup_{v \in \mathcal{W}} \frac{R_\mu(Z\alpha, v)}{\|v\|_{\mathcal{Y}}} \right) = \min_{\alpha \in \mathbb{R}^n} \| \boldsymbol{W}^\top \boldsymbol{R}_\mu(\boldsymbol{Z}\alpha) \|_2$$

Approximate minimum residual formulation ([TT, Zhang, 2021])

We introduce two successive approximations:

1. we replace $\sup_{v\in\mathcal{Y}}(\cdot)$ with $\sup_{v\in\mathcal{W}}(\cdot)$ where $\mathcal{W}=\operatorname{span}\{\psi_i\}_{i=1}^m$.

$$\min_{\alpha\in\mathbb{R}^n}\left(\sup_{v\in\mathcal{W}}\frac{R_\mu(Z\alpha,v)}{\|v\|_{\mathcal{Y}}}\right)=\min_{\alpha\in\mathbb{R}^n}\|\boldsymbol{W}^\top\boldsymbol{R}_\mu(\boldsymbol{Z}\alpha)\|_2$$

2. we replace the HF residual with the weighted residual

$$\min_{\alpha\in\mathbb{R}^n}\|\boldsymbol{W}^\top\boldsymbol{R}_\mu^{\mathrm{eq}}(\boldsymbol{Z}\alpha)\|_2=\sum_{i=1}^m\left(R_\mu^{\mathrm{eq}}(Z\alpha,\psi_i)\right)^2.$$

- The ROM reads as a nonlinear least-square problem with m eqs and n unknowns.
- The ROM does not explicitly depend on $\boldsymbol{Y}$.

Goal: exploit the linear analysis to inform the choice of $\mathcal{W}$ and $\mathbf{Y}$.

Consider the problem: find $u^\star \in \mathcal{X}$: $A(u^\star, v) = F(v) \qquad \forall\, v \in \mathcal{Y}$.

Define $\beta = \inf_{w\in\mathcal{X}} \sup_{v\in\mathcal{Y}} \dfrac{A(w,v)}{\|w\|_{\mathcal{X}}\|v\|_{\mathcal{Y}}}$, $\gamma = \sup_{w\in\mathcal{X}} \sup_{v\in\mathcal{Y}} \dfrac{A(w,v)}{\|w\|_{\mathcal{X}}\|v\|_{\mathcal{Y}}}$.

Introduce $\mathcal{Z} = \operatorname{span}\{\zeta_j\}_{j=1}^n \subset \mathcal{X}$, $\mathcal{W} = \operatorname{span}\{\psi_i\}_{i=1}^m \subset \mathcal{Y}$, and

and the LSPG ROM: $\hat{u} = \arg\min_{u\in\mathcal{Z}} \sup_{v\in\mathcal{W}} \dfrac{A(u,v) - F(v)}{\|v\|_{\mathcal{Y}}}$.

Goal: exploit the linear analysis to inform the choice of $\mathcal{W}$ and $\mathbf{Y}$.

Consider the problem: find $u^\star \in \mathcal{X}$: $A(u^\star, v) = F(v) \qquad \forall\, v \in \mathcal{Y}$.

Define $\beta = \inf_{w\in\mathcal{X}} \sup_{v\in\mathcal{Y}} \frac{A(w,v)}{\|w\|_{\mathcal{X}}\|v\|_{\mathcal{Y}}}$, $\gamma = \sup_{w\in\mathcal{X}} \sup_{v\in\mathcal{Y}} \frac{A(w,v)}{\|w\|_{\mathcal{X}}\|v\|_{\mathcal{Y}}}$.

Introduce $\mathcal{Z} = \operatorname{span}\{\zeta_j\}_{j=1}^n \subset \mathcal{X}$, $\mathcal{W} = \operatorname{span}\{\psi_i\}_{i=1}^m \subset \mathcal{Y}$, and

and the LSPG ROM: $\hat{u} = \arg\min_{u\in\mathcal{Z}} \sup_{v\in\mathcal{W}} \frac{A(u,v) - F(v)}{\|v\|_{\mathcal{Y}}}$.

Let $\mathcal{Y}^\star = \operatorname{span}\left\{R_{\mathcal{Y}}^{\text{riesz}} A(\zeta, \cdot) : \zeta \in \mathcal{Z}\right\}$, and $\delta_{n,m} = \inf_{s\in\mathcal{Y}^\star} \sup_{v\in\mathcal{W}} \frac{(s,v)_{\mathcal{Y}}}{\|s\|_{\mathcal{Y}}\|v\|_{\mathcal{Y}}}$.

Goal: exploit the linear analysis to inform the choice of $\mathcal{W}$ and $\mathbf{Y}$.

Consider the problem: find $u^\star \in \mathcal{X}$: $A(u^\star, v) = F(v) \qquad \forall\, v \in \mathcal{Y}$.

Define $\beta = \inf_{w\in\mathcal{X}} \sup_{v\in\mathcal{Y}} \frac{A(w,v)}{\|w\|_{\mathcal{X}}\|v\|_{\mathcal{Y}}}$, $\gamma = \sup_{w\in\mathcal{X}} \sup_{v\in\mathcal{Y}} \frac{A(w,v)}{\|w\|_{\mathcal{X}}\|v\|_{\mathcal{Y}}}$.

Introduce $\mathcal{Z} = \operatorname{span}\{\zeta_j\}_{j=1}^n \subset \mathcal{X}$, $\mathcal{W} = \operatorname{span}\{\psi_i\}_{i=1}^m \subset \mathcal{Y}$, and

and the LSPG ROM: $\hat{u} = \arg\min_{u\in\mathcal{Z}} \sup_{v\in\mathcal{W}} \frac{A(u,v) - F(v)}{\|v\|_{\mathcal{Y}}}$.

Let $\mathcal{Y}^\star = \operatorname{span}\left\{R_{\mathcal{Y}}^{\text{riesz}} A(\zeta, \cdot) : \zeta \in \mathcal{Z}\right\}$, and $\delta_{n,m} = \inf_{s\in\mathcal{Y}^\star} \sup_{v\in\mathcal{W}} \frac{(s,v)_{\mathcal{Y}}}{\|s\|_{\mathcal{Y}}\|v\|_{\mathcal{Y}}}$.

Error estimate: $\|\hat{u} - u^\star\|_{\mathcal{X}} \leq \frac{\gamma}{\beta} \frac{1}{\delta_{n,m}} \inf_{u\in\mathcal{Z}} \|u - u^\star\|_{\mathcal{X}}$.

Error estimate: $\|\hat{u} - u^\star\|_{\mathcal{X}} \leq \dfrac{\gamma}{\beta} \dfrac{1}{\delta_{n,m}} \inf_{u \in \mathcal{Z}} \|u - u^\star\|_{\mathcal{X}}$.

The space $\mathcal{W}$ should ensure that $\delta_{n,m}$ is close to one.

$\Rightarrow$ $\mathcal{W}$ should approximate the elements of $\mathcal{Y}^\star = \operatorname{span}\left\{R_{\mathcal{Y}}^{\text{riesz}} A(\zeta, \cdot) : \zeta \in \mathcal{Z}\right\}$.

The norm $\mathbf{Y}$ should ensure that $\dfrac{\gamma}{\beta}$ is close to one.

Error estimate: $\|\hat{u} - u^\star\|_{\mathcal{X}} \leq \dfrac{\gamma}{\beta} \dfrac{1}{\delta_{n,m}} \inf\limits_{u \in \mathcal{Z}} \|u - u^\star\|_{\mathcal{X}}$.

The space $\mathcal{W}$ should ensure that $\delta_{n,m}$ is close to one.
$\Rightarrow$ $\mathcal{W}$ should approximate the elements of $\mathcal{Y}^\star = \operatorname{span}\left\{R_{\mathcal{Y}}^{\text{riesz}} A(\zeta, \cdot) : \zeta \in \mathcal{Z}\right\}$.

The norm $\mathbf{Y}$ should ensure that $\dfrac{\gamma}{\beta}$ is close to one.

Practical algorithms

- construction of $\mathcal{W}$: Taddei, Zhang, 2021.
  see also Dahmen et al. M2AN, 2014; de Parga et al. CMAME, 2023.
- construction of $\mathbf{Y}$: Farhat, Iollo, Taddei, Telib, *in preparation*.
  see also Brunken et al., SISC, 2019; Edel,Maday, M3AS, 2023.

Choice of $\mathbf{Y}$ (I)

Linear problem: $u^\star \in \mathcal{X}: \quad A(u^\star, v) = F(v) \qquad \forall\, v \in \mathcal{Y}.$

LSPG ROM: $\hat{u} = \arg\min_{u \in \mathcal{Z}} \sup_{v \in \mathcal{W}} \dfrac{A(u,v) - F(v)}{\|v\|_{\mathcal{Y}}}.$

Error analysis: $\|\hat{u} - u^\star\|_{\mathcal{X}} \leq \boxed{\dfrac{\gamma}{\beta}} \dfrac{1}{\delta_{n,m}} \inf_{u \in \mathcal{Z}} \|u - u^\star\|_{\mathcal{X}}.$

Idea: choose $(\cdot,\cdot)_{\mathcal{Y}}$ to ensure $\frac{\gamma}{\beta} = 1$. $\Rightarrow \boldsymbol{Y} = \boldsymbol{A}\boldsymbol{X}^{-1}\boldsymbol{A}^\top$.

Choice of $\mathbf{Y}$ (I)

Linear problem: $u^\star \in \mathcal{X} : \quad A(u^\star, v) = F(v) \qquad \forall\, v \in \mathcal{Y}.$

LSPG ROM: $\hat{u} = \arg\min_{u \in \mathcal{Z}} \sup_{v \in \mathcal{W}} \dfrac{A(u, v) - F(v)}{\|v\|_{\mathcal{Y}}}.$

Error analysis: $\|\hat{u} - u^\star\|_{\mathcal{X}} \leq \boxed{\dfrac{\gamma}{\beta}} \dfrac{1}{\delta_{n,m}} \inf_{u \in \mathcal{Z}} \|u - u^\star\|_{\mathcal{X}}.$

Idea: choose $(\cdot, \cdot)_{\mathcal{Y}}$ to ensure $\frac{\gamma}{\beta} = 1$. $\Rightarrow \boldsymbol{Y} = \boldsymbol{A}\boldsymbol{X}^{-1}\boldsymbol{A}^\top$.

- The definition is based on the algebraic formulation
$\Rightarrow$ independent of the numerical scheme.

- The same idea has been exploited in several works.
PDE analysis: Lions, Magenes, "transposition method", 1972.

MOR: Dahmen et al, 2014; Brunken et al., 2019; Edel&Maday, 2023.

- The choice of $\boldsymbol{Y}$ cannot be extended to parametric problems.

Choice of $\mathbf{Y}$ (II): our (suboptimal) choices

Goal: determine the norm matrix $\boldsymbol{Y}$ for the nonlinear parametric problem: $\boldsymbol{R}_\mu(\boldsymbol{u}_\mu) = 0$.

1. Natural norm: $\boldsymbol{Y} = \overline{\boldsymbol{A}}\boldsymbol{X}^{-1}\overline{\boldsymbol{A}}^\top$, where $\overline{\boldsymbol{A}} = \boldsymbol{J}_{\bar{\mu}}[\boldsymbol{u}_{\bar{\mu}}]$.

2. A priori choice: exploit the variational formulation of the PDE to devise appropriate norms.

- *Incompressible flows:* H^1 norm for velocity, L^2 norm for pressure.
- *Conservation laws in divergence form* $\nabla \cdot F(u) = S(u)$: $\mathcal{Y} = H^1$.

Choice of $\mathbf{Y}$ (II): our (suboptimal) choices

Goal: determine the norm matrix $\boldsymbol{Y}$ for the nonlinear parametric problem: $\boldsymbol{R}_\mu(\boldsymbol{u}_\mu) = 0$.

1. Natural norm: $\boldsymbol{Y} = \overline{\boldsymbol{A}}\boldsymbol{X}^{-1}\overline{\boldsymbol{A}}^\top$, where $\overline{\boldsymbol{A}} = \boldsymbol{J}_{\bar{\mu}}[\boldsymbol{u}_{\bar{\mu}}]$.

Pros: exploits already-available tools of the code; provable optimality for $\mu = \bar{\mu}$.

Cons: expensive to evaluate.

2. A priori choice: exploit the variational formulation of the PDE to devise appropriate norms.

- *Incompressible flows:* H^1 norm for velocity, L^2 norm for pressure.
- *Conservation laws in divergence form* $\nabla \cdot F(u) = S(u)$: $\mathcal{Y} = H^1$.

Pro: less expensive to evaluate;

Cons: more involved implementation for non-standard formulations.

Model problem (I): nozzle flow

Define $u = \begin{bmatrix} A\rho \\ A\rho v \\ AE \end{bmatrix}$, $F(u) = \begin{bmatrix} A\rho v \\ A(\rho v^2 + p) \\ Au(E + p) \end{bmatrix}$ and $S(u) = \begin{bmatrix} 0 \\ p\partial_x A \\ 0 \end{bmatrix}$ with

$A(x) = 3 + 4(A_0 - 3)\frac{x}{L}\left(1 - \frac{x}{L}\right)$, $L = 10$.

Consider the conservation law $\partial_x F(u) = S(u)$ in $(0, L)$ with parameters $\mu = [A_0, p_0]$.

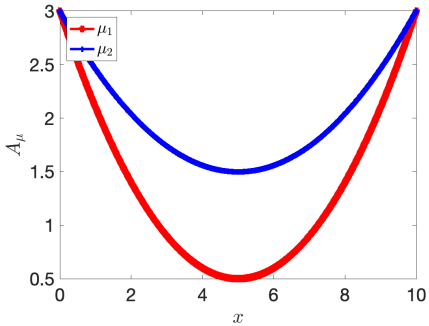

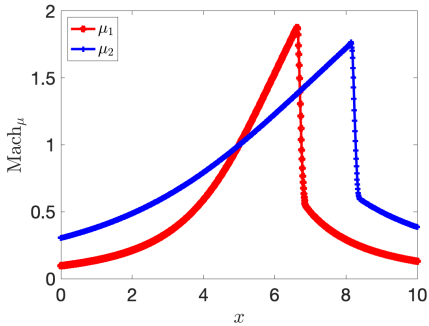

Model problem (II): array of LS89 blades

Model: compressible Euler equations in subsonic regime ($\gamma = 1.4$).

Parameters: distance between blades, far-field Mach number.

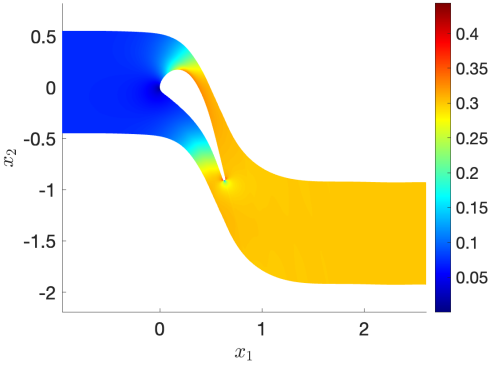

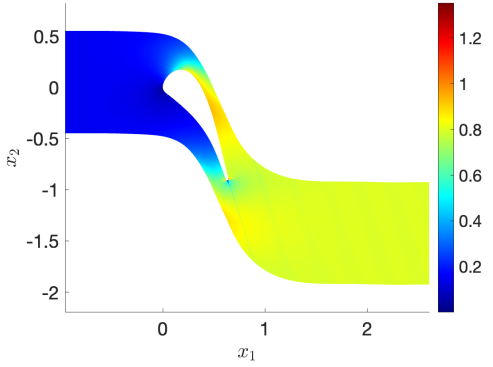

Results (I): nozzle flow

Relative error: $\frac{\|\widehat{u}_\mu - u_\mu^{\mathrm{hf}}\|}{\|u_\mu^{\mathrm{hf}}\|}$; **suboptimality index:** $\frac{\|\widehat{u}_\mu - u_\mu^{\mathrm{hf}}\|}{\min_{u \in \mathcal{Z}} \|u_\mu^{\mathrm{hf}} - u\|}$.

Goal: assess the choice of the norm $\mathbf{Y}$ – "natural" refers to the choice of Farhat et al.

All results are averaged over 25 out-of-sample parameters.

L^2 error			
n_{train}	L^2	natural	H^1
5	0.0589	0.0302	0.0300
10	0.0387	0.0126	0.0128
15	0.0309	0.0071	0.0113
20	0.0336	0.0045	0.0149
25	0.0280	0.0029	0.0106
30	0.0356	0.0022	0.0080
35	0.0235	0.0012	0.0053
40	0.0305	0.0036	0.0072

suboptimality index			
n_{train}	L^2	natural	H^1
5	3.0	1.4	1.4
10	8.9	1.6	1.8
15	14.2	2.2	3.9
20	34.2	2.1	12.8
25	68.1	2.1	16.0
30	79.1	1.9	10.9
35	69.7	2.1	9.7
40	93.7	2.6	8.9

Results (II): array of LS89 blades

L^2 error			
n_{train}	L^2	natural	H^1
5	0.0036	0.0009	0.0010
10	0.0007	0.0003	0.0004
15	0.0005	0.0002	0.0003
20	0.0003	0.0002	0.0002

suboptimality index			
n_{train}	L^2	natural	H^1
5	4.9	1.0	1.2
10	3.2	1.1	1.7
15	3.1	1.1	1.6
20	2.7	1.1	1.5

Model reduction of parametric conservation laws

- Least-square Petrov-Galerkin projection
- Lagrangian approximations

Nonlinear approximations (I): inadequacy of linear methods

State-of-the-art MOR methods rely on

- linear approximations, $\widehat{u}_\mu = Z\,\widehat{\alpha}_\mu$, with Z linear operator;

- a single high-fidelity discretization to represent *all* elements of the solution set $\mathcal{M} = \{u_\mu : \mu \in \mathcal{P}\}$.

State-of-the-art MOR methods rely on

- linear approximations, $\widehat{u}_\mu = Z\,\widehat{\alpha}_\mu$, with Z linear operator;

  Linear approximations are inadequate for transport phenomena.

- a single high-fidelity discretization to represent *all* elements of the solution set $\mathcal{M} = \{u_\mu : \mu \in \mathcal{P}\}$.

  Mesh adaptation is needed to resolve sharp features.

Technical issue: slow decay of Kolmogorov n-width.

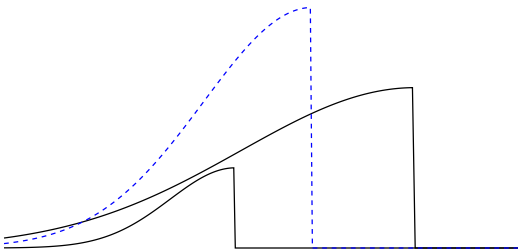

Illustration courtesy of M Zahr (Univ. Notre Dame).

Nonlinear approximations (I): inadequacy of linear methods

State-of-the-art MOR methods rely on

- linear approximations, $\widehat{u}_\mu = Z\,\widehat{\alpha}_\mu$, with Z linear operator;

  Linear approximations are inadequate for transport phenomena.

- a single high-fidelity discretization to represent *all* elements of the solution set $\mathcal{M} = \{u_\mu : \mu \in \mathcal{P}\}$.

  Mesh adaptation is needed to resolve sharp features.

Technical issue: slow decay of Kolmogorov n-width.

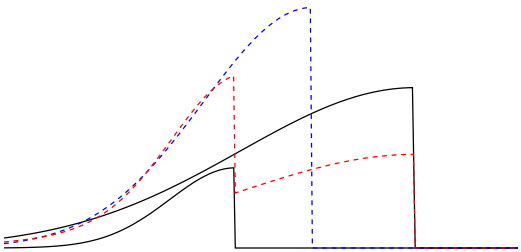

Illustration courtesy of M Zahr (Univ. Notre Dame).

Nonlinear approximations (II): construction of the reduced-order basis

Nonlinear MOR techniques rely on nonlinear low-rank approximations Z.

Several options have been proposed in the literature.

Nonlinear approximations (II): construction of the reduced-order basis

Nonlinear MOR techniques rely on nonlinear low-rank approximations Z.

Several options have been proposed in the literature.

- **Affine:** $Z(\alpha) = \bar{u} + Z_1\alpha$;
- **Piecewise:** $Z_\mu(\alpha) = \sum_{i=1}^{\kappa} \chi_{\mathcal{P}_i}(\mu) Z_i \alpha$; Eftang et al, 2010; Amsallem et al, 2012.
- **Augmented:** $Z(\alpha) = Z_1\alpha + Z_2 f(\alpha)$, $f : \mathbb{R}^n \to \mathbb{R}^m$ nonlinear; Barnett&Farhat, 2022; Barnett et al, 2023.
- **Lagrangian:** $Z(\alpha, a) = Z_1\alpha \circ \mathtt{N}(a)^{-1}$, $\mathtt{N}(a) : \Omega \to \Omega$ bijection; Ohlberger&Rave, 2013; Iollo&Lombardi, 2014; ...
- **Multi-frame:** $Z(\alpha, a) = \sum_{i=1}^{\kappa} Z_i \alpha_i \circ \mathtt{N}(a_i)$, $\mathtt{N}(a) : \Omega \to \mathbb{R}^d$; Reiss et al, 2018; .
- **Autoencoders:** $Z(\alpha) = \mathfrak{N}(\alpha)$, $\mathfrak{N} : \mathbb{R}^n \to \mathcal{X}$ autoencoder. Lee&Carlberg, 2020.

Nonlinear approximations (III): Lagrangian methods

The choice of the nonlinear ansatz is a compromise between **expressivity** and **learnability**.

- **Expressivity of Z:** $\min_{\alpha \in \mathbb{R}^n} \|u_\mu - Z(\alpha)\| \leq \texttt{tol} \quad \forall\, \mu \in \mathcal{P}$, for moderate n.
- **Learnability:** offline costs of finding Z; online costs and robustness of the ROM.

The choice of the nonlinear ansatz is a compromise between **expressivity** and **learnability**.

- **Expressivity of Z:** $\min_{\alpha \in \mathbb{R}^n} \|u_\mu - Z(\alpha)\| \leq \texttt{tol} \ \ \forall\, \mu \in \mathcal{P}$, for moderate n.
- **Learnability:** offline costs of finding Z; online costs and robustness of the ROM.

Observation: for relevant problems in continuum mechanics, coherent structures — e.g., shocks, shear layers, cracks — vary smoothly with the parameter.

Implication: there exists a low-rank mapping $\Phi : \Omega \times \mathcal{P} \to \Omega$ such that the *mapped solution set* $\widetilde{\mathcal{M}} = \{u_\mu \circ \Phi_\mu \ : \ \mu \in \mathcal{P}\}$

- is amenable for linear compression (e.g., POD),
- can be represented through a single HF discretization.

The problem of finding the mapping Φ based on snapshots of $\mathcal{M} = \{u_\mu \ : \ \mu \in \mathcal{P}\}$ is referred to as *registration problem*.

Lagrangian ansatz: replace the linear ansatz $\widehat{u}_\mu = Z\widehat{\alpha}_\mu$ with $\widehat{u}_\mu = \widetilde{u}_\mu \circ \Phi_\mu^{-1}$, where $\widetilde{u}_\mu = Z\widehat{\alpha}_\mu, \quad \Phi_\mu = \mathtt{N}(\widehat{a}_\mu)$.

- The composition with Φ_μ^{-1} corresponds to a mesh deformation.

  $\Rightarrow$ *easy to implement for FE/FV discretizations*

- The action Φ_μ^{-1} should track sharp features of the solution field.

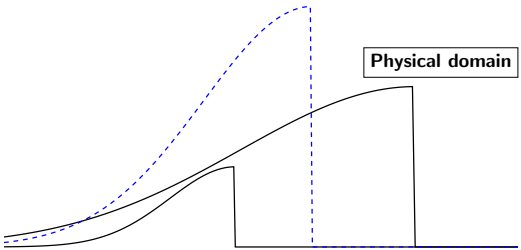

Goal: devise an integrated MOR formulation for Lagrangian approximations.

Lagrangian ansatz: replace the linear ansatz $\widehat{u}_\mu = Z\widehat{\alpha}_\mu$ with $\widehat{u}_\mu = \widetilde{u}_\mu \circ \Phi_\mu^{-1}$, where $\widetilde{u}_\mu = Z\widehat{\alpha}_\mu, \quad \Phi_\mu = \mathtt{N}(\widehat{a}_\mu)$.

- The composition with Φ_μ^{-1} corresponds to a mesh deformation.

  $\Rightarrow$ *easy to implement for FE/FV discretizations*

- The action Φ_μ^{-1} should track sharp features of the solution field.

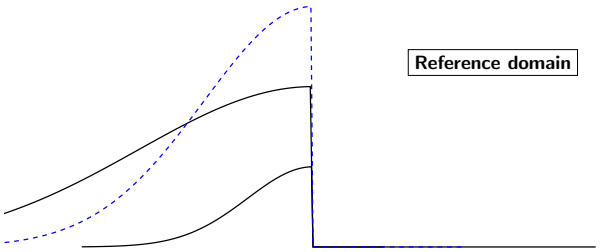

Goal: devise an integrated MOR formulation for Lagrangian approximations.

General procedure: ingredients and specific tasks

Lagrangian ansatz: $\widehat{u}_\mu = \widetilde{u}_\mu \circ \Phi_\mu^{-1}$ with $\widetilde{u}_\mu = Z\widehat{\alpha}_\mu, \quad \Phi_\mu = \mathtt{N}(\widehat{a}_\mu)$.

Discrete representation: consider a *nodal-based* discretization on the mesh $\mathcal{T}_{\mathrm{hf}}$

- the FE field u is defined by $\mathcal{T}_{\mathrm{hf}}$ and the vector $\mathbf{u} \in \mathbb{R}^N$ of nodal evaluations;
- given the bijection Φ, denote by $\Phi(\mathcal{T}_{\mathrm{hf}})$ the deformed mesh.

Then, the Lagrangian ansatz reads as $\mu \mapsto (\Phi_\mu(\mathcal{T}_{\mathrm{hf}}), \mathbf{Z}\widehat{\alpha}_\mu)$.

Key observation: The ansatz is linear wrt $\widehat{\alpha}_\mu$, highly-nonlinear wrt Φ_μ.

General procedure: ingredients and specific tasks

Lagrangian ansatz: $\widehat{u}_\mu = \widetilde{u}_\mu \circ \Phi_\mu^{-1}$ with $\widetilde{u}_\mu = Z\widehat{\alpha}_\mu$, $\Phi_\mu = \mathbb{N}(\widehat{a}_\mu)$.

Discrete representation: consider a *nodal-based* discretization on the mesh $\mathcal{T}_{\mathrm{hf}}$

- the FE field u is defined by $\mathcal{T}_{\mathrm{hf}}$ and the vector $\mathbf{u} \in \mathbb{R}^N$ of nodal evaluations;
- given the bijection Φ, denote by $\Phi(\mathcal{T}_{\mathrm{hf}})$ the deformed mesh.

Then, the Lagrangian ansatz reads as $\mu \mapsto (\Phi_\mu(\mathcal{T}_{\mathrm{hf}}), \mathbf{Z}\widehat{\alpha}_\mu)$.

Key observation: The ansatz is linear wrt $\widehat{\alpha}_\mu$, highly-nonlinear wrt Φ_μ.

Basic tasks:

Registration problem: find the parametric bijection Φ.

Mesh adaptation: find the mesh $\mathcal{T}_{\mathrm{hf}}$ for the solution set $\widetilde{\mathcal{M}} = \{u_\mu \circ \Phi_\mu : \mu \in \mathcal{P}\}$.

Model reduction: determine the ROB Z and the ROM for $\widehat{\alpha}$ to estimate the solution to the parametric PDE.

General offline training procedure: [Barral,TT,Tifouti, JCP,2024]

Initialization: $\Phi^{(0)} = \mathtt{id}$, $\mathcal{P}_{\text{train}} \subset \mathcal{P}$, $\mathcal{T}_{\text{hf}}^{(0)} = \mathcal{T}_{\text{hf}}^{(1)}$.

`For` $k = 1, \ldots, N_{\text{it}}$

1. Snapshot generation $\quad \mathcal{T}_{\text{hf}}^{(k-1)} \Rightarrow \mathcal{S}^{(k-1)} = \{u_\mu^{\text{hf},(k-1)} : \mu \in \mathcal{P}_{\text{train}}\}$
2. `if` $k > 1$, Parametric mesh adaptation $\quad \mathcal{S}^{(k-1)} \Rightarrow \mathcal{T}_{\text{hf}}^{(k)}$
3. Registration $\quad \left(\mathcal{S}^{(k-1)}, \mathcal{T}_{\text{hf}}^{(k)}\right) \Rightarrow \Phi^{(k)}$
4. MOR training $\quad \left(\Phi^{(k)}, \mathcal{T}_{\text{hf}}^{(k)}\right) \Rightarrow \left(Z^{(k)}, \text{ROM}^{(k)}\right)$

`EndFor`

General offline training procedure: [Barral,TT,Tifouti, JCP,2024]

Initialization: $\Phi^{(0)} = \texttt{id}$, $\mathcal{P}_{\text{train}} \subset \mathcal{P}$, $\mathcal{T}_{\text{hf}}^{(0)} = \mathcal{T}_{\text{hf}}^{(1)}$.

`For` $k = 1, \ldots, N_{\text{it}}$

1. Snapshot generation $\quad \mathcal{T}_{\text{hf}}^{(k-1)} \Rightarrow \mathcal{S}^{(k-1)} = \{u_\mu^{\text{hf},(k-1)} : \mu \in \mathcal{P}_{\text{train}}\}$
2. `if` $k > 1$, Parametric mesh adaptation $\quad \mathcal{S}^{(k-1)} \Rightarrow \mathcal{T}_{\text{hf}}^{(k)}$
3. Registration $\quad \left(\mathcal{S}^{(k-1)}, \mathcal{T}_{\text{hf}}^{(k)}\right) \Rightarrow \Phi^{(k)}$
4. MOR training $\quad \left(\Phi^{(k)}, \mathcal{T}_{\text{hf}}^{(k)}\right) \Rightarrow \left(Z^{(k)}, \text{ROM}^{(k)}\right)$

`EndFor`

- The for loop addresses inaccuracy of early-stage HF simulations;
- MOR training can be performed using standard linear MOR methods for parametric geometries;
- information from previous iterations needs to be re-used to speed up the training phase. not covered in this talk.

Inviscid flow past an array of LS89 blades

Steady-state compressible Euler equations for ideal gases ($\gamma = 1.4$).

Challenges: periodic BCs; several coherent structures (shock, wakes), geometry parameterization.

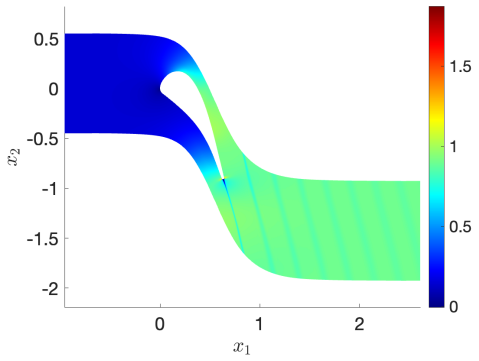

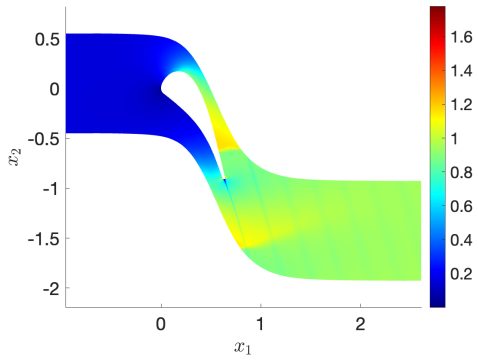

Inviscid flow past an array of LS89 blades

Steady-state compressible Euler equations for ideal gases ($\gamma = 1.4$).

Challenges: periodic BCs; several coherent structures (shock, wakes), geometry parameterization.

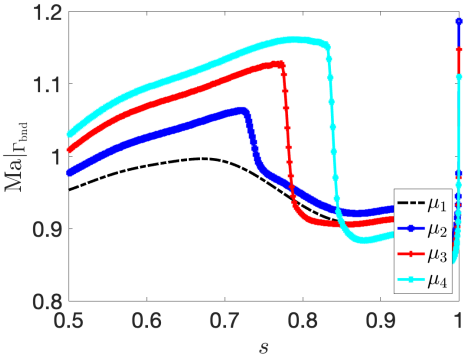

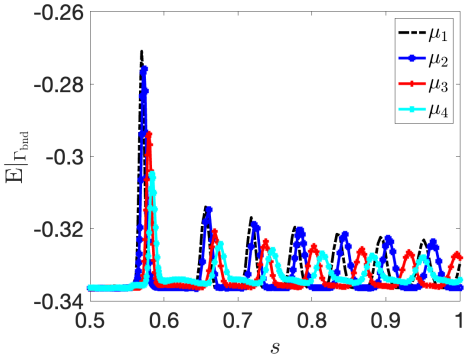

Description of the test

We perform $N_{\text{it}} = 3$ iterations of the adaptive procedure.

- We consider a P2 DG discretization with dilation-based AV.

  Yu, Hesthaven, CiCP, 2020.

- Snapshot generation is performed using the available ROM from the previous iteration.
- We validate performance over $n_{\text{test}} = 20$ out-of-sample parameters.

Description of the test

We perform $N_{\text{it}} = 3$ iterations of the adaptive procedure.

- We consider a P2 DG discretization with dilation-based AV.

  Yu, Hesthaven, CiCP, 2020.

- Snapshot generation is performed using the available ROM from the previous iteration.
- We validate performance over $n_{\text{test}} = 20$ out-of-sample parameters.

Metrics

L^2 relative error: $E_\mu^{\text{hf}} = \dfrac{\|u_\mu^{\text{hf}} - \widehat{u}_\mu\|_{L^2(\Omega)}}{\|u_\mu^{\text{hf}}\|_{L^2(\Omega)}}$;

L^2 sub-optimality index: $\eta_\mu^{\text{hf}} = \dfrac{\|u_\mu^{\text{hf}} - \widehat{u}_\mu\|_{L^2(\Omega)}}{\min_{\zeta \in \mathcal{Z}_n} \|u_\mu^{\text{hf}} - \zeta\|_{L^2(\Omega)}}$;

error in total enthalpy: $E_\mu^{\infty} = \dfrac{\|H_\mu^{\text{hf}} - H_\mu^{\text{th}}\|_{L^2(\Omega)}}{\|H_\mu^{\text{th}}\|_{L^2(\Omega)}}$. HF error indicator.

Results (I): model reduction

We rely on

- LSPG projection with element/edge-wise EQ hyper-reduction;
- discretize-then-map (DtM) approach to handle geometry variations;
- greedy sampling driven by residual indicator $n(it) = [15, 17, 25]$.

Greedy sampling terminates when the relative error associated with the new snapshot is less than 0.1%.

Right: relative L^2 error.

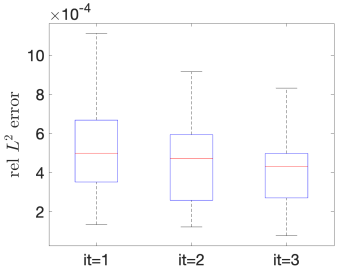

References: Carlberg et al., JCP, 2013; Farhat et al., IJNME 2015; Yano, ACOM 2019; Washabaugh et al., AIAA 2016; TT, Zhang, CMAME 2021; Veroy et al.. AIAA, 2003.

Results (I): model reduction

We rely on

- LSPG projection with element/edge-wise EQ hyper-reduction;
- discretize-then-map (DtM) approach to handle geometry variations;
- greedy sampling driven by residual indicator $n(it) = [15, 17, 25]$.

Greedy sampling terminates when the relative error associated with the new snapshot is less than 0.1%.

Right: sub-optimality index.

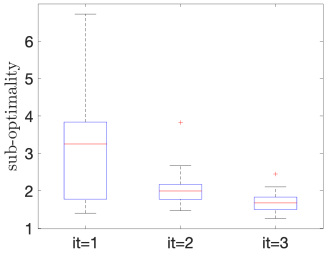

References: Carlberg et al., JCP, 2013; Farhat et al., IJNME 2015; Yano, ACOM 2019; Washabaugh et al., AIAA 2016; TT, Zhang, CMAME 2021; Veroy et al.. AIAA, 2003.

Results (I): model reduction

We rely on

- LSPG projection with element/edge-wise EQ hyper-reduction;
- discretize-then-map (DtM) approach to handle geometry variations;
- greedy sampling driven by residual indicator $n(it) = [15, 17, 25]$.

Greedy sampling terminates when the relative error associated with the new snapshot is less than 0.1%.

Right: enthalpy error.

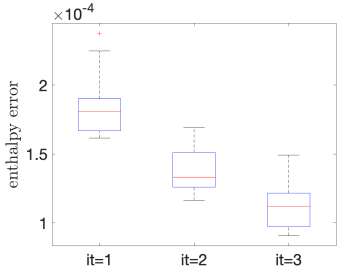

References: Carlberg et al., JCP, 2013; Farhat et al., IJNME 2015; Yano, ACOM 2019; Washabaugh et al., AIAA 2016; TT, Zhang, CMAME 2021; Veroy et al.. AIAA, 2003.

Results (I): model reduction

We rely on

- LSPG projection with element/edge-wise EQ hyper-reduction;
- discretize-then-map (DtM) approach to handle geometry variations;
- greedy sampling driven by residual indicator $n(it) = [15, 17, 25]$.

Greedy sampling terminates when the relative error associated with the new snapshot is less than 0.1%.

Right: wall-clock online cost.

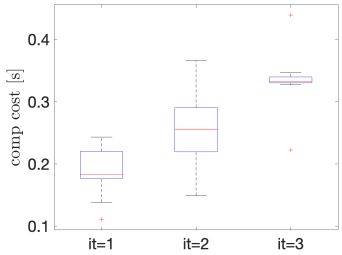

References: Carlberg et al., JCP, 2013; Farhat et al., IJNME 2015; Yano, ACOM 2019; Washabaugh et al., AIAA 2016; TT, Zhang, CMAME 2021; Veroy et al.. AIAA, 2003.

Registration is based on Mach number and four point sensors.

Figure (left): Mach number on the upper side of the blade.

Figure (right): Entropy on the lower boundary.

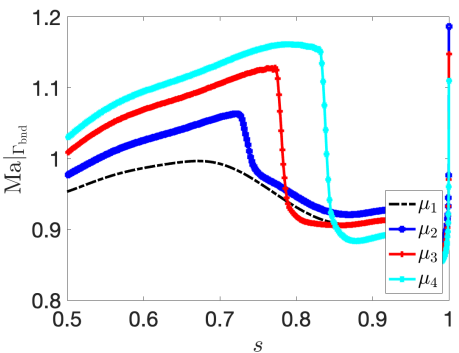

(a) phys config.

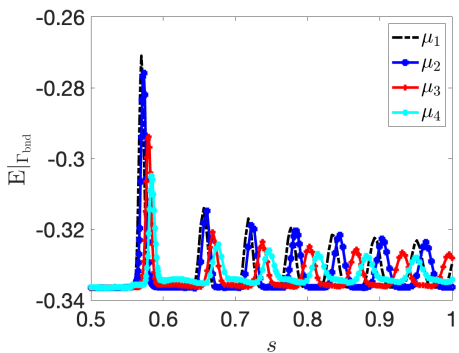

(b) phys config.

Registration is based on Mach number and four point sensors.

Figure (left): Mach number on the upper side of the blade.

Figure (right): Entropy on the lower boundary.

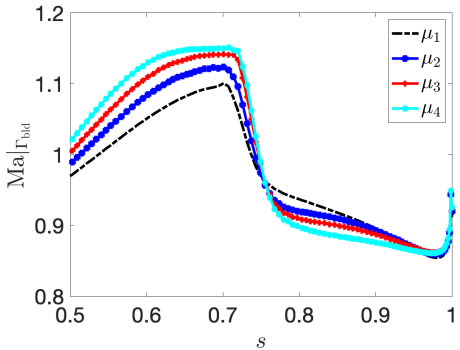

(a) reference config.

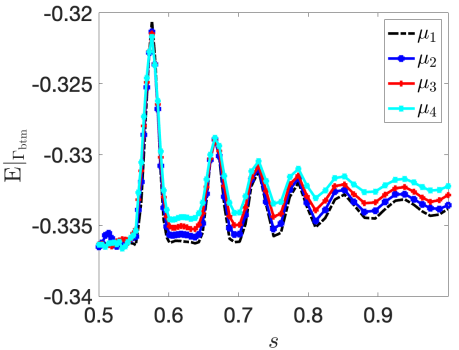

(b) reference config.

Registration is based on Mach number and four point sensors.

Figure (left): Mach number on the upper side of the blade.

Figure (right): Entropy on the lower boundary.

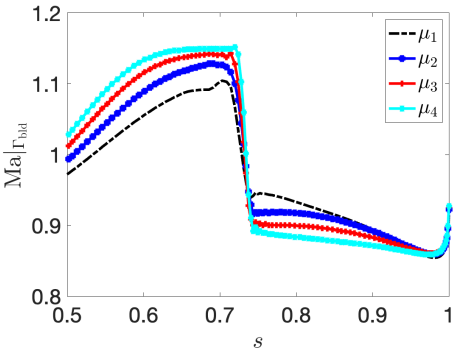

(a) reference config.

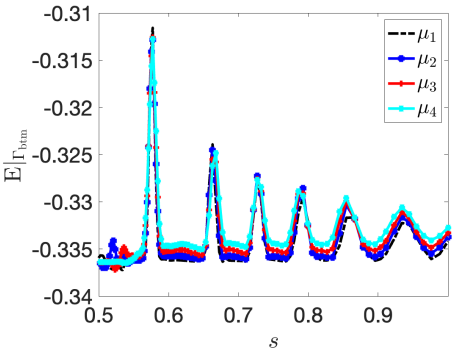

(b) reference config.

Results (II): registration (iteration 3)

Registration is based on Mach number and four point sensors.

Figure (left): Mach number on the upper side of the blade.

Figure (right): Entropy on the lower boundary.

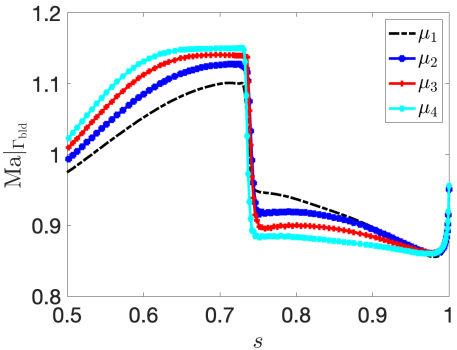

(a) reference config.

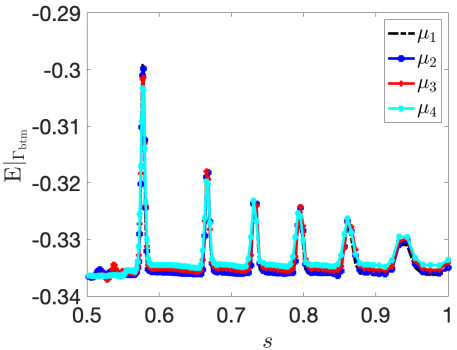

(b) reference config.

Results (III): mesh adaptation (iteration 1)

We rely on a mark-then-refine strategy driven by the local variation of total enthalpy and the norm of the gradient of the entropy.

Implementation is based on the Inria software MMG.

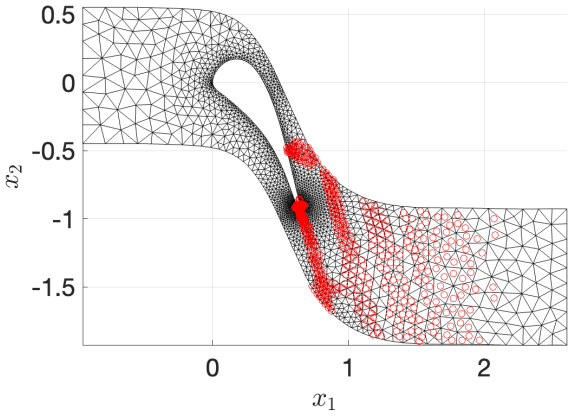

Results (III): mesh adaptation (iteration 2)

We rely on a mark-then-refine strategy driven by the local variation of total enthalpy and the norm of the gradient of the entropy.

Implementation is based on the Inria software MMG.

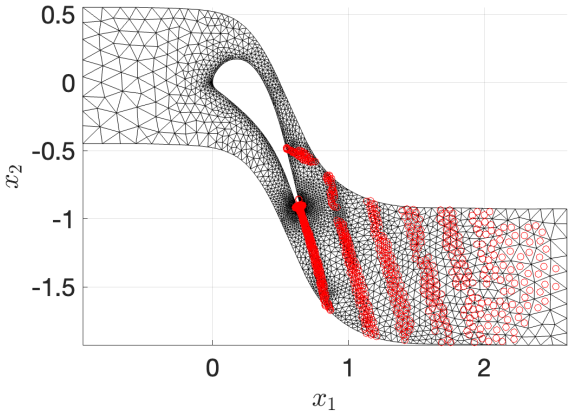

Results (III): mesh adaptation (iteration 3)

We rely on a mark-then-refine strategy driven by the local variation of total enthalpy and the norm of the gradient of the entropy.

Implementation is based on the Inria software MMG.

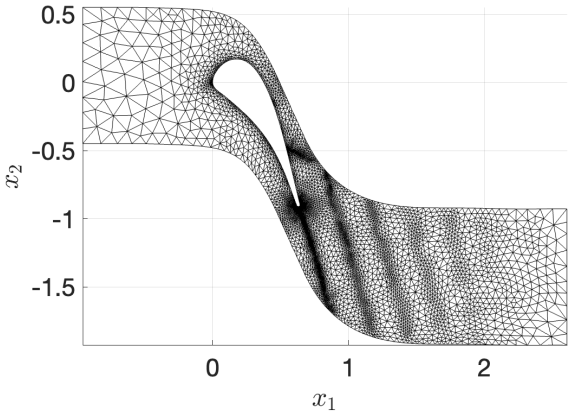

Results (III): mesh adaptation (iteration 3)

We rely on a mark-then-refine strategy driven by the local variation of total enthalpy and the norm of the gradient of the entropy.

Implementation is based on the Inria software MMG.

Interpretation: we rely on two separate mesh adaptation mechanisms:

- parameter-independent *h*-refinement;
- parameter-dependent *r*-refinement based on registration.

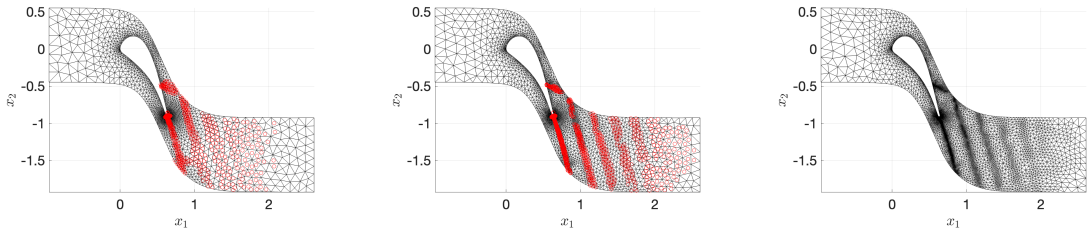

Results (IV): offline computational costs (total 5h 33')

Percentage of offline costs of the last greedy algorithm : $\approx 72\%$.
$\Rightarrow$ offline costs comparable with state-of-the-art linear method.

	it = 1	it = 2	it = 3
ROB size:	15	17	25
mesh elements:	4249	7398	13396
snapshot generation:	1213.35	12.07	14.82
registration (sensor def.):	139.00	153.25	167.22
registration (optimization):	304.52	423.77	1147.62
mesh adaptation:	0.00	3.53	1.45
greedy alg (HF solves):	226.90	1457.03	12899.77
greedy alg (overhead):	87.65	313.90	1446.37
PTC iterations (avg):	6.40	18.18	51.88

Conclusions

Summary

We propose a projection-based ROM for steady conservation laws based on **LSPG projection** and **Lagrangian approximations**.

Summary

We propose a projection-based ROM for steady conservation laws based on **LSPG projection** and **Lagrangian approximations**.

The choice of the weighting norm plays a major role in the performance of LSPG ROMs

- the H^1 norm performs fairly well
- the "natural" norm is considerably more accurate, at the price of larger offline costs.

Summary

We propose a projection-based ROM for steady conservation laws based on **LSPG projection** and **Lagrangian approximations**.

The choice of the weighting norm plays a major role in the performance of LSPG ROMs

- the H^1 norm performs fairly well
- the "natural" norm is considerably more accurate, at the price of larger offline costs.

Lagrangian approximations provide a good compromise between expressivity and learnability.

Extension: piecewise Lagrangian approximations to deal with shock-topology changes.
Barral, TT, Tifouti, AIAA, 2025

Registration methods for the construction of the mapping still require many advances.

Thank you for your attention

For more information, visit the website:

math.u-bordeaux.fr/~ttaddei/ .

Backup slides

Preliminary (I): residual decomposition

Consider the FE mesh $\mathcal{T}_{\mathrm{hf}}$ of Ω with elements $\{\mathrm{D}_k\}_{k=1}^{N_{\mathrm{e}}}$, nodes $\{x_j^{\mathrm{hf}}\}_{j=1}^{N_{\mathrm{v}}}$ and facets $\{\mathrm{F}_j\}_{j=1}^{N_{\mathrm{f}}}$.

The residual can be decomposed as follows:

$$\mathfrak{R}(u,v) = \sum_{k=1}^{N_{\mathrm{e}}} r_k^{\mathrm{e}}(u_k, v_k) + \sum_{j=1}^{N_{\mathrm{f}}} r_j^{\mathrm{f}}(u_j^+, u_j^-, v_j^+, v_j^-),$$

where $\{r_k^{\mathrm{e}}\}_k$ and $\{r_j^{\mathrm{f}}\}_j$ are local operators.

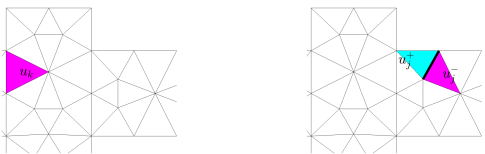

The decomposition is consistent with typical FE assembly routines.

Residual evaluation is accelerated by resorting to a reduced quadrature:

$$\mathfrak{R}_\mu^{\mathrm{eq}}(u,v) = \sum_{k=1}^{N_{\mathrm{e}}} \rho_k^{\mathrm{e,eq}} r_k^{\mathrm{e}}(u_k, v_k) + \sum_{j=1}^{N_{\mathrm{f}}} \rho_j^{\mathrm{f,eq}} r_j^{\mathrm{f}}(u_j^+, u_j^-, v_j^+, v_j^-),$$

where $\boldsymbol{\rho}^{\mathrm{e,eq}} \in \mathbb{R}_+^{N_{\mathrm{e}}}$, $\boldsymbol{\rho}^{\mathrm{f,eq}} \in \mathbb{R}_+^{N_{\mathrm{f}}}$ are sparse.

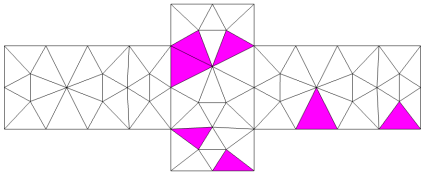

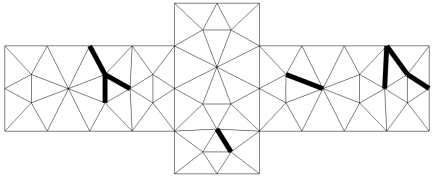

Refs: *reduced integration domain* (Ryckelynck, 2005); *mesh sampling and weighting* (Farhat et al., 2015); *empirical cubature* (Hernández et al., 2017); *empirical quadrature procedures* (Yano, Patera, 2019).

Remark: several alternatives are available (e.g., elementwise residual; pointwise residual).

Analogy: $A(\zeta, \cdot)$ corresponds to $DR_\mu[u_\mu](\zeta, \cdot)$ for nonlinear problems.

We choose $\mathcal{W}$ to approximate the fields $R_{\mathcal{Y}}^{\text{riesz}}\left(DR_\mu[u_\mu](\zeta_i, \cdot)\right)$ for all $i = 1, \ldots, n$ and $\mu \in \mathcal{P}$.

Practical algorithm: given the snapshots $\{u_\mu : \mu \in \mathcal{P}_{\text{train}}\}$,

1. compute $\mathfrak{Y}_{\text{train}} = \left\{ \boldsymbol{Y}^{-1} \boldsymbol{J}_\mu[\boldsymbol{u}_\mu]\boldsymbol{\zeta}_i \ : \ i = 1, \ldots, n, \mu \in \mathcal{P}_{\text{train}} \right\}$;
2. apply POD to $\mathfrak{Y}_{\text{train}}$ with inner product $(\cdot, \cdot)_{\mathcal{Y}}$;
3. choose m based on an energy criterion.

Recall that $\boldsymbol{Y}^{-1} \boldsymbol{J}_\mu[\boldsymbol{u}_\mu]\boldsymbol{\zeta}_i$ *is the algebraic counterpart of* $R^{\text{riesz}} DR_\mu[u_\mu](\zeta_i, \cdot)$

Analogy: $A(\zeta, \cdot)$ corresponds to $DR_\mu[u_\mu](\zeta, \cdot)$ for nonlinear problems.

We choose $\mathcal{W}$ to approximate the fields $R_{\mathcal{Y}}^{\text{riesz}}\left(DR_\mu[u_\mu](\zeta_i, \cdot)\right)$ for all $i = 1, \ldots, n$ and $\mu \in \mathcal{P}$.

Practical algorithm: given the snapshots $\{u_\mu : \mu \in \mathcal{P}_{\text{train}}\}$,

1. compute $\mathfrak{Y}_{\text{train}} = \left\{ \boldsymbol{Y}^{-1} \boldsymbol{J}_\mu[\boldsymbol{u}_\mu]\boldsymbol{\zeta}_i \ : \ i = 1, \ldots, n, \mu \in \mathcal{P}_{\text{train}} \right\}$;
2. apply POD to $\mathfrak{Y}_{\text{train}}$ with inner product $(\cdot, \cdot)_{\mathcal{Y}}$;
3. choose m based on an energy criterion.

The space $\mathcal{W}$ is built during the offline stage.

$\Rightarrow$ The method can cope with arbitrary non-diagonal $\boldsymbol{Y}$.

Recall that $\boldsymbol{Y}^{-1} \boldsymbol{J}_\mu[\boldsymbol{u}_\mu]\boldsymbol{\zeta}_i$ *is the algebraic counterpart of* $R^{\text{riesz}} DR_\mu[u_\mu](\zeta_i, \cdot)$

Question: how does the choice of the norm affect the "complexity" of the optimization problem?

(Partial) answer: the Gauss-Newton method exhibits similar performance for the three choices of $\mathbf{Y}$.

Nozzle problem			
n_{train}	L^2	natural	H^1
5	6.8	10.3	7.6
10	6.4	9.2	8.2
15	6.6	21.7	6.9
20	9.6	8.8	6.5
25	7.4	9.7	8.9
30	9.4	8.6	14.0
35	9.6	6.9	8.2

LS89 blade			
n_{train}	L^2	natural	H^1
5	3.7	3.4	3.3
10	3.8	3.4	3.3
15	3.4	3.2	3.0
20	3.4	3.2	3.0